Langmuir

Article

pubs.acs.org/Langmuir

Interaction Forces between DPPC Bilayers on Glass

Raquel Orozco-Alcaraz and Tonya L. Kuhl*

Department of Chemical Engineering and Materials Science, University of California—Davis, One Shields Avenue, Davis California 95616, United States

Supporting Information

ABSTRACT: The surface force apparatus (SFA) was utilized to obtain force−distance profiles between silica-supported membranes formed by Langmuir−Blodgett deposition of 1,2-dipalmitoyl-*sn*-glycero-3-phosphocholine (DPPC). In the absence of a membrane, a long-range electrostatic repulsion and short-range steric repulsion are measured as a result of the deprotonation of silica in water and the roughness of the silica film. The electrostatic repulsion is partially screened by the lipid membrane, and a van der Waals adhesion comparable to that measured with well-packed DPPC membranes on mica is measured. This finding suggest that electrostatic interactions due to the underlying negatively charged silica are likely present in other systems of glass-supported membranes. In contrast, the charge of an underlying mica substrate is almost completely screened when a lipid membrane is deposited on the mica. The difference in the two systems is attributed to the stronger physisorption of zwitterionic lipids to molecularly smooth mica compared to physisorption to rougher silica.

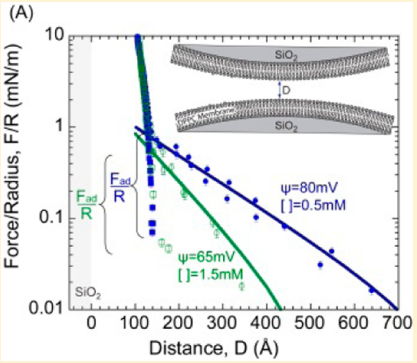

INTRODUCTION

Because of the complexity of cell membranes, biophysical studies have primarily focused on model membrane systems of reduced complexity in order to elucidate the fundamental thermodynamics and physics of membrane interactions. For example, lipids and their self-organizing structures have been broadly used as models of cellular membranes and have been studied for their potential use in biosensor applications.[1] In this work, we compare the interaction forces between supported membranes composed of one of the most commonly studied phospholipids, DPPC on two different supports: molecularly smooth but chemically inert mica versus more functional and broadly used silica or glass.

There are a plethora of techniques used to study membranes; however, relatively few provide a measure of membrane−membrane interactions.[2,3] One of the first methods developed relied on changes in the spacing between membranes in multilamellar stacks under osmotic stress to extract the repulsive interactions between membranes.[4,5] Such studies provided an unprecedented understanding of the role of membrane undulations and hydration. The use of small- and wide-angle X-ray and neutron scattering also provided high-resolution density distributions and the average packing of lipids in the membrane to be obtained.[6−9] More recently, the bioforce probe based on the micropipet aspiration of giant unilamellar vesicles has been used to measure membrane−membrane interactions. Initially used to study membrane tension and area compressibility by measuring changes in membrane shape as a function of pipet suction pressure, the use of opposing membranes and/or a force-sensing red blood cell expanded the measuring capability to detect weak attractive interactions as well as biological specificity interactions such as ligand−receptor binding.[2,10−12] In terms of substrate-supported membranes, atomic force microscopy (AFM)[13] is widely used to measure membrane topology but is only sparingly used to measure membrane−membrane interactions due to challenges in forming a membrane on silicon nitride tips.[14−16] Chemically functionalizing the tip with gold and a hydrophobic mercapto undecanol has been shown to promote spontaneous vesicle fusion, yielding a supported lipid monolayer appropriate for measuring membrane−membrane interactions.[15]

The most widely used and versatile technique for measuring membrane−membrane interactions is the surface force apparatus, which provides force−distance profiles with 1 Å resolution in distance and 10 pN resolution in force and a visualization of the area of contact between two macroscopic membrane-coated surfaces.[2,17−22] Traditionally, SFA employs mica, a molecularly smooth and widely used solid support for force spectroscopy and fluorescence microscopy measurements. However, membrane-based biosensors typically use silica or glass substrates, in part because of the fact that silica is readily available, cheap, easily chemically modified, optically transparent, and less sensitive to surface damage.[23−25] It is thus important to establish the typical conditions present (e.g., charge density, hydrophobicity, steric interactions, etc.) for a bilayer immobilized on silica and thus how a silica-supported membrane interacts with materials in the environment (e.g., particles, proteins, cells, etc.) for applications. Moreover, there is a large effort to develop models to recapitulate integral membrane proteins in supported membranes for controlled

Received: October 2, 2012
Revised: November 25, 2012
Published: November 30, 2012

biophysical studies.[26−28] To study the interaction of membranes with transmembrane proteins, it is necessary to prevent deleterious interactions of the embedded protein with the underlying inorganic support. Hydrophilic polymer cushions are actively being pursued as a means to provide a highly hydrated, soft, flexible spacer between the substrate and the membrane to mimic biological conditions and native function better.[24,29−40] The grafting of polymers on silica is becoming routine. Our future work will present studies of interaction forces of polymer-cushioned membranes.[41]

Though the interaction between lipid bilayers immobilized on mica surfaces have been well documented, no work has reported measurements of membranes immobilized on silica using the SFA. In this work, we measure and analyze the interaction between two DPPC bilayers deposited on smooth silica thin films. Silica (SiO_2) is deposited via electron beam deposition (e-beam) on mica to yield relatively smooth films (5 Å rms). The resulting optical interferometer is analyzed using both the five-layer multiple-beam interferometry analytical solution and a multiple matrix solution of the full optical system (Supporting Information). The results are compared to the interaction of bilayers immobilized directly on mica under similar conditions.

MATERIALS AND METHODS

Chemicals. 1,2-Dipalmitoyl-*sn*-glycero-3-phosphocholine (DPPC) (melting point 41 °C) was purchased from Avanti Polar Lipids, Inc. (Alabaster, AL). Texas red 1,2-dihexadecanoyl-sn-glycero-3-phosphoethanolamine, triethylammonium salt (Texas red DHPE) was purchased from Life Technologies Corp. (Grand Island, NY). Lipids were dissolved in chloroform at a concentration of 1 mg/mL. KNO_3 was used as the monovalent salt in all solutions. The water used was purified with a Milli-Q gradient water purification system with a resistivity of 18 MΩ·cm.

Sample Preparation. Silica-covered mica was prepared on the basis of the procedures previously described by Vigil et al.[42] First, mica was cleaved to uniform thicknesses of 3 to 4 μm and adhered to a clean mica backing sheet. A CHA e-beam evaporator (SEC-600-RAP) was then used to deposit SiO_2 onto the mica pieces. To ensure uniform deposition, the samples were rotated in their planetaries, and the raster was scanned at an amplitude of one-fourth of the crucible's diameter. Films with approximately 500 Å or 1000 Å SiO_2 layers were deposited using the following operating conditions; base pressure of 10^{-6} Torr, deposition pressure of 5×10^{-6} Torr, filament current of 26 mA, acceleration voltage of −10 kV, and deposition rate of ∼1 Å/s. After the SiO_2 was deposited, the SiO_2-covered mica pieces were flipped and adhered to a clean mica sheet and silver was evaporated onto the back side of the mica pieces. Samples were stored under vacuum in this configuration until use.

Supported lipid bilayers were prepared by Langmuir−Blodgett (LB) deposition using a temperature-controlled Wilhelmy trough (Nima Coventry, U.K.) and assembled onto the back-silvered mica or SiO_2-covered mica substrates glued onto cylindrical silica disks via a procedure described elsewhere.[43,44] Prior to lipid deposition, the SiO_2−mica surfaces were placed under UV light for a total of 30 min in 10 min increments to ensure cleanliness and surface hydroxylation. Both the inner and outer leaflets of DPPC were deposited at 45 mN/m. The inner leaflet was deposited by raising the substrates vertically through a compressed DPPC monolayer at the air−water interface at a dipping speed of 1 mm/min. The monolayer transfer ratio was 1.00 ± 0.05 on mica and 0.97 ± 0.05 on SiO_2−mica. Subsequently, the outer DPPC layer was deposited in vertical geometry under similar conditions but at a faster deposition rate of 4 mm/min to prevent the desorption of the inner leaflet at the air−water interface. The transfer ratio for the outer monolayer was 1.00 ± 0.05 on mica and 0.90 ± 0.05 on SiO_2−mica. The pressure−area isotherms obtained were in agreement with those in the literature.[45] To demonstrate the similar quality of the deposited DPPC membranes on mica and SiO_2−mica surfaces, fluorescent images of DPPC membranes containing 1 mol % Texas red DHPE are shown in the Supporting Information. No fluorescent dye was incorporated into membranes for SFA experiments.

Atomic Force Microscopy (AFM). AFM studies were carried out using the NEAT-ORU spectral imaging facility on the UC Davis campus with an Asylum Research (Santa Barbara, CA) MFP-3D AFM. Veeco silicon nitride MSCT levers, $k \approx 0.03$, were used for imaging.

Surface Force Measurements. The SFA technique has been used extensively to measure interaction forces between surfaces.[46,47] After bilayers were deposited on the solid support, the surfaces were transferred and mounted into the SFA under water, a procedure detailed elsewhere.[17] The water in the SFA box was saturated with a speck of DPPC to prevent lipid desorption from the substrates during the course of the measurements. After the surfaces were mounted, the SFA box was placed in a temperature-controlled room at 25.0 °C. A custom automated SFA was used for convenient data collection.[48] The system enables constant and/or variable motor displacements via a computer-controlled motor system. A sensitive CCD camera (Princeton SPEC-10:2K Roper Scientific, Trenton, NJ) was interfaced with the spectrometer and computer acquisition system to allow automated wavelength determination of the fringes of equal chromatic order.

The separation distance analysis traditionally used for supported membranes on mica surfaces is to approximate the system as a symmetric three-layer interferometer and use analytical solutions for the resulting optical interferometer. Other methods include a five-layer analytical form and the multilayer matrix model (MMM) that can be used for asymmetric and more complicated optical systems. Immobilizing bilayers on mica-covered silica surfaces requires an extra set of symmetric layers in the interferometer and complicates the analysis of the separation distance. In the Supporting Information for this work, we demonstrate that approximating the optical system using a simple three-layer interferometer is insufficient and can be used only as a first estimate of the separation distance. The difference between the results obtained using the three-layer analytical method and MMM is ∼13%, and the difference between the five-layer analytical method and MMM is ∼3.5% for separation distances of less than 200 Å. In this work, the five-layer analytical method was primarily employed. The membrane thickness at contact was determined using MMM.

RESULTS

AFM of SiO_2-Covered Mica. Figure 1A shows a representative AFM image of an ∼1000-Å-thick SiO_2 layer

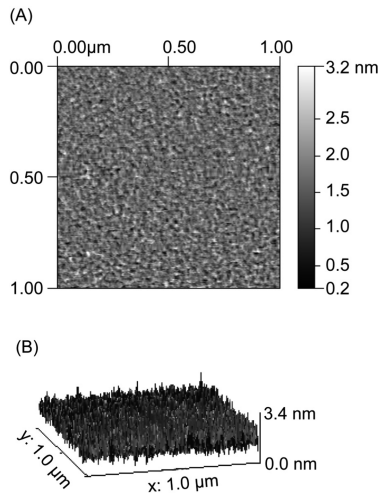

Figure 1. (A) Representative 1 μm × 1 μm AFM scan of a SiO_2 e-beam-evaporated film on mica in Milli-Q water. (B) Three-dimensional profile of A. The peak-to-valley roughness of the film is 31 ± 2 Å.

dx.doi.org/10.1021/la3039329 | *Langmuir* 2013, 29, 337−343

that was e-beam deposited on mica hydrated in Milli-Q water. Figure 1B shows the 3D profile that corresponds to image 1A. Image analysis gave a peak-to-valley roughness of 31 ± 2 Å for a hydrated film in bulk water (6 ± 2 Å rms). Similar surface quality was observed with dry films in air (results not shown). In all cases, scans were recorded over different regions of the films, and the scans were reproducible. Similar but lower values of the roughness of e-beam-deposited SiO_2 thin films on mica were reported by Vigil et al. The surface quality of our films is also consistent with SFA measurements, where we found that the SiO_2 films swelled slightly by 2.2% in water compared to their dry thickness (Supporting Information). Vigil et al. suggested that the swelling was due to the formation of protruding silica hairs or gel formation at the SiO_2−water interface. Because the roughness of our SiO_2 film did not increase appreciably upon hydration, we attribute the 2.2% increase in film thickness to imbibing a small amount of water in defects within the SiO_2 film.

SiO_2 Interaction in Aqueous Solution. Figure 2 shows the force−distance profile between two e-beam-evaporated silica films on mica in ~0.5 mM KNO_3 at pH 6. The contact, D = 0, was defined as a hard, flattened contact in air ($F/R \geq 70$ mN/m). The force curve is characterized by two types of repulsive interactions: the expected long-range electrostatic double-layer interaction due to the negative charge of the silica film in water and a shorter-range steric interaction presumably due to surface roughness and hydration.[49,50] Theoretically and experimentally, both electrostatic and steric/hydration interactions decay roughly exponentially. The silica surfaces were assumed to be symmetric (i.e., the films had the same negative charge density or surface potential). The electrostatic interaction was then fitted by solving the nonlinear Poisson−Boltzmann (P−B) equation using a numerical algorithm developed by Grabbe and Horn.[51] The algorithm explicitly computes the electrostatic potential or constant surface charge between two flat surfaces using a relaxation method on a finite mesh. The Derjaguin approximation was used to convert from the energy between flats to the force between crossed cylinders, $F/R = 2\pi E$. The solid lines are the P−B fits for a constant potential of $\psi = -107$ mV and a constant surface charge of σ = 9.2 mC/m^2. These results are in good agreement with previous studies where the magnitude of the negative surface potential of silica at pH 7.5 was $\psi = -120$ mV in 0.1 mM NaCl.[23,52] For the conditions here, pH ~6, a lower charge density and zeta potential are expected.[53]

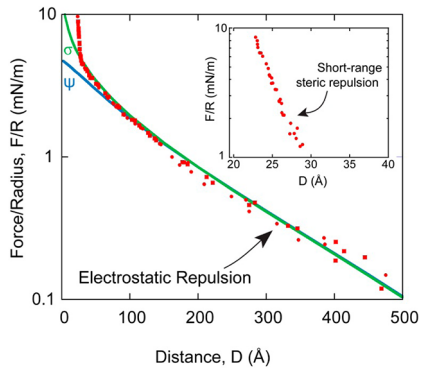

Figure 2. Force−distance profile between two e-beam-evaporated silica films on mica substrates in ~0.5 mM KNO_3. Solid lines are electrostatic fits to the data using the Poisson−Boltzmann (P−B) equation with constant surface potential $\psi = -107$ mV and constant surface charge $\sigma = -9.2$ mC/m^2. D = 0 is defined as a hard, flattened contact between the silica films (F/R > 70 mN/m) submerged in water. (Inset) Remaining steric force after subtracting the electrostatic contribution.

To qualify the short-range interaction better, the electrostatic contribution was subtracted from the measured force profile.[43] The remaining steric portion of the interaction is shown in the inset of Figure 2. The measured force profile deviates from a purely electrostatic interaction at short range, D < 30 Å, consistent with the AFM topography measurements in Figure 1. When an exponential is fit to $F/R \approx \exp(D/L_c)$, we find that the characteristic length for this case is $L_c \approx 6$ Å. The characteristic length is consistent with the hydration of the silica interface and the compression/interdigitation of protrusions of the opposing surfaces (6 ± 2 Å rms).[49,50] Valtiner et al. previously suggested that this additional force was due to repulsive hydration and steric forces.[54,55] After hydration, no change in the interaction profile was detected over many days, demonstrating that the films were stable. A similar short-range repulsion between silica films in water was observed by Vigil et al.[42] but was attributed to the extension of dangling Si−(−O−Si−)$_n$−OH groups and the formation of a silica gel.

Control Measurements of DPPC Bilayers on Mica. Traditionally, DPPE has been used as the inner leaflet layer in supported membrane experiments measured with the SFA. DPPE binds to mica through a strong electrostatic interaction and provides a stable hydrophobic surface upon which to deposit the outer lipid monolayer leaflet. Here, a symmetric DPPC bilayer was used instead because DPPC is one of the most commonly studied phospholipids and is considered to be a better mimic of biological membranes.[23,56] Before describing the results of the force−distance, $F(D)$, measurements, it is important to establish an appropriate reference framework for the contact between the bilayer surfaces, which will be defined as D = 0. As in previous SFA measurements, we choose to define D = 0 as the contact between membranes in the absence of hydration and protrusion effects.[17] In the case of DPPC membranes supported on mica, the hydrated thickness of the two outer monolayers, Δ, was determined at the end of each experiment by measuring the thickness change following the drainage of the solution from the apparatus and the removal of the two outer monolayers. From the measured thickness change relative to contact between the bilayers at a force of about 10 mN/m, the bilayer−bilayer contact, D = 0, was defined as

$$D = \Delta - T \tag{1}$$

The anhydrous bilayer thickness (T) was calculated from the known volumes occupied by the hydrocarbon chains and PC headgroup given by

$$T = \frac{2(2V_{hc} + V_{head})}{A} \tag{2}$$

where V_{hc} = (27.4 + 26.9n) Å^3 is the average volume of a saturated n-carbon chain in the gel state,[57] V_{head} = 324.5 Å^3 is the average headgroup volume of PC,[58] and A is the deposited area per lipid. For example, the thickness of two outer DPPC monolayers deposited at A = 48 Å^2 per molecule (Π = 45 mN/m) is $T = 2[2(27.4 + 26.9 \times 15) + 324.5]/48 = 49.4$ Å. Typically, phosphotidylcholine membranes come into contact at separations of about 20−30 Å depending on the compressive load.[17,59] The thickness of the bilayer was assumed to remain

dx.doi.org/10.1021/la3039329 | Langmuir 2013, 29, 337−343

constant during the experiments. This is reasonable given that the DPPC monolayers (T_{mp} = 41 °C) were deposited at room temperature in a close-packed solid phase and no phase changes or density changes are expected to take place.

Figure 3A shows the measured force−distance profile between two DPPC bilayers immobilized on mica substrates

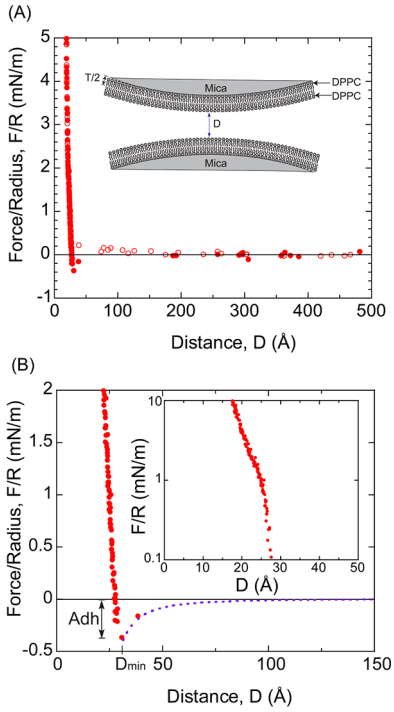

Figure 3. (A) Force−distance profile between two DPPC bilayers supported on mica in a monovalent solution of 0.5 mM KNO_3. Open circles indicate the approach, and solid circles indicate the separation. (Inset) Illustration of the experimental system, where D = 0 is defined as the contact between two nonhydrated DPPC bilayers. T is the thickness of a DPPC bilayer. (B) Small-range plot of the data in A showing the van der Waals interaction $F = -AR/6D^2$ (dashed line) with $A = (7 \pm 1) \times 10^{-21}$ J. A_{dh} is the magnitude of adhesion force. (Inset) Semilogarithmic plot of the repulsive portion of the force profile.

in a monovalent solution of 0.5 mM KNO_3 at room temperature. As can be seen, a very weak repulsion[60] is observed between the surfaces for separations below ~150 Å, followed by a strong, short-range repulsion at about 30 Å. Because DPPC is zwitterionic but overall neutral, we attribute the weak repulsion to a small level of residual charge from the mica surfaces or lipid membrane because the decay length is roughly consistent with the electrolyte concentration.[60] If fully dissociated, mica has a maximum surface charge density[46] of 50 $Å^2/e^-$. The surface charge density or surface potential measured experimentally is dependent upon the type and concentration of electrolyte present in the solution. As shown in Figure 3A, the surface charge on mica is almost completely damped after depositing a bilayer (with a low dielectric oil core) on the surface.[61] The almost-negligible electrostatic repulsion suggests reasonably strong electrostatic binding of the DPPC lipid bilayer to mica. The electrostatic binding arises from the attractive interaction between the underlying, negatively charged mica substrate and the positively charged terminus of the zwitterionic headgroup. In contrast, no electrostatic repulsion is measured when the inner leaflet of the membrane is DPPE. Presumably, the difference resides in the weaker physisorption and higher hydration of PC headgroups compared to those of PE headgroups.[62]

Figure 3B illustrates the van der Waals adhesion between the DPPC bilayers with a magnitude of $A_{dh} = F_{ad}/R = -0.40 \pm 0.10$ mN/m at a separation of D = 30 ± 3 Å. In addition, the experimental data were compared to the theoretical van der Waals (VDW) interaction[17] $F = -AR/6D^2$ (dashed line) with $A = (7 \pm 1) \times 10^{-21}$ J, with excellent agreement. The inset in Figure 3B is a semilogarithmic plot of the short-range repulsion between the membranes. An ever-present hydration layer on the headgroups and the thermal protrusions of lipids from the membrane are responsible for the short-range repulsion. In addition, as suggested Marra and Israelachvili,[17] the hydration of cations can also add to the repulsive force.

SFA Measurements of DPPC Bilayers Immobilized on SiO_2. The measured transfer ratio of the DPPC bilayer on the SiO_2-coated mica surfaces was 0.97 ± 0.05 for the inner leaflet and 0.90 ± 0.05 for the outer leaflet. This result corroborates an earlier reflectivity study that showed the formation of a well-packed membrane with nearly complete coverage on a silica surface using the LB deposition technique.[63] Fluorescent images of DPPC membranes containing 1 mol % Texas red DHPE on SiO_2-coated mica are shown in the Supporting Information. As evidenced by fluorescence microscopy, well-packed membranes are present on the micrometer scale. However, the presence of small defects cannot be ruled out from such measurements. The lower transfer ratios of lipid monolayers obtained on silica to mica also suggest that the membranes on silica contain a higher number of defects, which is consistent with the significant electrostatic repulsion measured with silica-supported DPPC membranes as described in the next section. Bassereau and Pincet demonstrated that lipids in the inner leaflet can desorb during the deposition of the outer leaflet monolayer, thereby resulting in lower transfer ratios and holes in the bilayer. The holes span the thickness of the bilayer because of the high energy of exposing hydrophobic chains to water. The adsorption energy of a DPPC lipid to SiO_2 versus mica can be readily estimated from its transfer ratio using[64]

$$\frac{E_a}{kT} = \frac{\alpha a_m \gamma_{DPPC}}{kT} - \ln(\rho) \qquad (3)$$

where E_a is the adsorption energy, k is the Boltzmann constant, T is the temperature, a_m is the molecular area of DPPC (a_m= 45 $Å^2$ at Π_{DPPC} = 45 mN/m),[65,66] α is a correlation coefficient, and γ_{DPPC} is the surface tension of DPPC at the air−water interface defined as γ_{DPPC} = 72 mN/m − Π_{DPPC}.[67] The ratio between the total surface covered by holes and the bilayer is $\rho = x/(1-x)$, where x can be found from the transfer ratio $x = (1 - TR)/2$.[64] To calculate the adhesion energy, we assume α = 0.7, the correlation value measured for DMPE on mica.[64] This yields an adsorption energy of a DPPC bilayer on silica of $E_a \approx 1kT$ (for TR = 0.90) versus an adsorption energy on mica of $E_{a,min} > 3kT$ (for TR = 0.99). This difference confirms the lower adsorption energy of DPPC bilayers on silica than on mica.

Figure 4A shows the measured force−distance profile of DPPC bilayers immobilized on silica substrates at different ionic strengths (0.5 and 1.5 mM KNO_3). The reduction of the long-range repulsion with increased salt concentration clearly demonstrates that the interaction is electrostatic. As mentioned earlier, the headgroups of the lipid bilayers are zwitterionic but overall neutral in charge. Thus, the long-range electrostatic

dx.doi.org/10.1021/la3039329 | Langmuir 2013, 29, 337−343

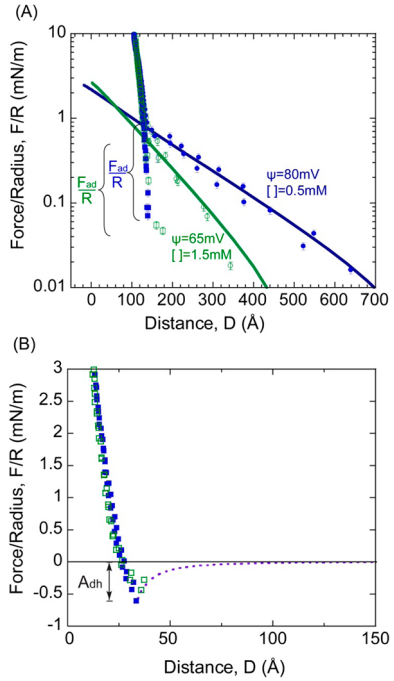

Figure 4. (A) Measured force profile between DPPC–DPPC membranes supported on SiO_2–covered mica in 0.5 mM and 1.5 mM KNO_3. D = 0 is defined as contact between bare SiO_2–SiO_2 surfaces in 0.5 mM KNO_3. (B) Force profile after the electrostatics have been subtracted from the measured force profile in A. D = 0 is based on the contact between two nonhydrated DPPC bilayers. The dashed line is the theoretical van der Waals fit ($F = -AR/6D^2$). $A_{dh} = F_{ad}/R$ is the magnitude of the adhesion force.

force is due to the underlying, negatively charged SiO_2-coated mica substrates. To delineate the electrostatic contribution of the SiO_2 films in the measured force profile clearly, the reference frame, D = 0, is based on the SiO_2–SiO_2 contact in a 0.5 mM KNO_3 aqueous solution rather than DPPC–DPPC membrane contact. The distance shift was based on the contact before (SiO_2–SiO_2 in water) and after the bilayers were immobilized on silica using MMM to determine the thickness of the membranes. MMM was used in this case to ensure correct membrane thickness measurements. Equation 1 was also employed to observe consistency in the outer-layer thickness between immobilized bilayers on silica versus mica. Interestingly, we observed an additional shift of 20 Å in the thickness estimated by draining the SFA of water and the removal of the outer DPPC monolayer leaflets compared to studies on mica. We attribute this to some loss of the inner-layer leaflets of the membranes immobilized on silica. The removal of more than the outer two leaflets demonstrates a weaker physisorption of the inner leaflet to silica as compared to mica, again consistent with the difference in the estimated adsorption energy (eq 3).

The electrostatic repulsion was fit using the Poisson–Boltzmann (P–B) equation at the two salt concentrations. The electrostatic potential decreases slightly as the electrolyte concentration increases, and the potential is lower in the presence of a membrane (Figure 2). The significant electrostatic repulsion is likely due to small holes in the membrane and therefore less screening of the underlying substrate charge by the supported membrane. Adhesion is again observed when the surfaces are separated. The adhesion is comparable between the two salt concentrations with a magnitude of about −0.65 mN/m. This is in very good agreement with the expected VDW adhesion between DPPC bilayers.[17] No additional attraction or adhesion from hydrophobic interactions was detected. This is consistent with the formation of membrane-spanning holes as observed by AFM.[64,68,69] We further comment that the measured adhesion is identical to the measured adhesion of DPPC membranes on mica once the small electrostatic contribution is accounted for, −(0.40 + 0.20) mN/m.

After subtracting the electrostatic contribution (Figure 4B), we found that the remaining short-range repulsion is "softer" compared to when the bilayer is supported on mica substrates. This softer repulsion is consistent with the increase in surface roughness.[54,55] In this figure, D = 0 was defined as the contact between DPPC bilayers for ease of comparison to the data shown in Figure 3. To obtain D = 0, the thickness of two DPPC membranes was determined using eq 2 and subtracted from the total thickness as determined using MMM and the contact wavelengths in the presence and absence of the membranes.

CONCLUSIONS

Though the interactions between lipid bilayers immobilized on mica surfaces have been well documented, much less work has been done on bilayers immobilized on silica. The closest system was the measurement of a lipid bilayer on mica with a bare silica surface by Anderson et al.[23] The measured profile between a mica-supported membrane and bare silica surface demonstrated that a long-range repulsion force, attributed to the residual double-layer potential, and short-range repulsive thermal undulation forces were the dominant interactions.

The structure of DPPC membranes is similar on mica and silica surfaces as ascertained by fluorescence microscopy (Supporting Information); however, it is likely that silica-supported membranes contain more holes as indicated by reduced transfer ratios. The measured forces between DPPC bilayers immobilized on silica or mica are also similar, with the exception of a stronger electrostatic repulsive force present when silica is used. A summary of the forces and observations made in these experiments is enumerated next. First, the most important difference between the interaction of bilayers immobilized on mica and bilayers immobilized on silica is the presence of a strong electrostatic force when silica is used. We attribute this force to holes in silica-supported membranes due to the weaker physisorption of lipids to the silica substrate and the hydrated surface roughness of the silica. These defects are below the resolution of fluorescence microscopy. Second, a van der Waals attraction consistent with well-packed membranes is measured upon membrane separation. In Figures 3B and 4B, the theoretical van der Waals interaction, $F = -AR/6D^2$ with $A = (7 \pm 1) \times 10^{-21}$ J is plotted against the experimental results (dashed lines for both figures). For silica, the adhesive minimum is at $D_{adh} = 34 \pm 3$ Å, which is slightly greater than the distance for mica ($D_{adh} = 30 \pm 3$ Å) as a result of the greater fluctuations in the more hydrated membrane and the roughness of the underlying silica support. The magnitude of the adhesion force between membranes immobilized on silica, A_{dh}, is in agreement with theoretical predictions and previous measurements of DPPC membranes supported on inner leaflets of DPPC.[17] The adhesion is comparable between the two salt concentrations at about 0.65 mN/m. Third, membranes on silica appear to be slightly more compressible because of the softer/rougher underlying silica layer. Fourth, the physisorption of the inner DPPC leaflet to silica is weaker than to mica and

dx.doi.org/10.1021/la3039329 | Langmuir 2013, 29, 337–343

can be quantified by the lower transfer ratios during Langmuir–Blodgett deposition.

In particular, the presence of an unexpected electrostatic interaction when membranes are supported on silica and the presence of holes in the membrane could be important in biophysical membrane studies on glass and biosensor applications where the selective binding of ligands or proteins to membranes is important.

■ ASSOCIATED CONTENT

Supporting Information

Experimental comparison of the multilayer matrix model to the three- and five-layer multiple-beam interferometry models. Fluorescence microscopy images of supported DPPC membranes on mica and silica-coated mica. This material is available free of charge via the Internet at http://pubs.acs.org

■ AUTHOR INFORMATION

Corresponding Author

*E-mail: tlkuhl@ucdavis.edu.

Notes

The authors declare no competing financial interest.

■ ACKNOWLEDGMENTS

This work was supported by the NSF chemistry division through grant CHE-0957868 and by an NIH training grant in biomolecular technology awarded by the designated emphasis in biotechnology at UC Davis. We also thank Daniel Kienle and Dennis Mulder for assistance with MMM modeling, William Chan for fluorescence microscopy measurements, and Gwen Schuman for her contributions to transfer ratio measurements.

■ REFERENCES

(1) Sackmann, E. Supported Membranes: Scientific and Practical Applications. *Science* **1996**, *271*, 43–48.

(2) Leckband, D.; Israelachvili, J. Intermolecular Forces in Biology. *Q. Rev. Biophys.* **2001**, *34*, 105–267.

(3) Claesson, P. M.; Ederth, T.; Bergeron, V.; Rutland, M. W. Techniques for Measuring Surface Forces. *Adv. Colloid Interface Sci.* **1996**, *67*, 119–183.

(4) Rand, R P.; Parsegian, V.A. Hydration Forces between Phospholipid Bilayers. *Biochim. Biophys. Acta* **1989**, *988*, 351–376.

(5) Safinya, C. R.; Roux, D.; Smith, G. S.; Sinha, S. K.; Dimon, P.; Clark, N. A.; Bellocq, A. M. Steric Interactions in a Model Multimembrane System: A Synchrotron X-ray Study. *Phys. Rev. Lett.* **1986**, *57*, 2718–2721.

(6) Parsegian, V. A.; Fuller, N.; Rand, R. P. The Role of Long Range Forces in Ordered Arrays of Tobacco Mosaic Virus. *Nature* **1979**, *259*, 632–635.

(7) Caffrey, M. B.; Bilderback, D. H. Realtime X-ray Diffraction Using Synchrotron Radiation: System Characterization and Applications. *Nucl. Instrum. Methods* **1983**, *208*, 495–510.

(8) Nagle, J. F.; Tristam-Nagle, S. Structure of Lipid Bilayers. *Biochim. Biophys. Acta* **2000**, *1469*, 159–195.

(9) Petrache, H. I.; Gouliaev, N.; Tristram-Nagle, S.; Zhang, R.; Suter, R. M. Interbilayer Interactions from High-Resolution X-ray Scattering. *Phys. Rev. E* **1998**, *57*, 7014–7024.

(10) Evans, E.; Klingenberg, D. J.; Rawicz, W.; Szoka, F. Interactions between Polymer-Grafted Membranes in Concentrated Solutions of Free Polymer. *Langmuir* **1996**, *12*, 3031–3037.

(11) Evans, E.; Needham, D. Physical Properties of Surfactant Bilayer Membranes: Thermal Transitions, Elasticity, Rigidity, Cohesion, and Colloidal Interactions. *J. Phys. Chem.* **1987**, *91*, 4219–4228.

(12) Evans, E.; Ritchie, K. Sensitive Force Technique to Probe Molecular Adhesion and Structural Linkages at Biological Interfaces. *Biophys. J.* **1995**, *68*, 2580–2587.

(13) Alessandrini, A.; Facci, P. AFM: A Versatile Tool in Biophysics. *Meas. Sci. Technol.* **2005**, *16*, R65–R92.

(14) Garcia-Manyes, S.; Sanz, F. Nanomechanics of Lipid Bilayers by Force Spectroscopy with AFM: A Perspective. *Biochim. Biophys. Acta* **2010**, *1798*, 741–749.

(15) Pera, I.; Stark, R.; Kappl, M.; Butt, H.-J.; Benfenati, F. Using the Atomic Force Microscope to Study the Interaction between Two Solid Supported Lipid Bilayers and the Influence of Synapsin I. *Biophys. J.* **2004**, *87*, 2446–2455.

(16) Richter, R. P.; Brisson, A. Characterization of Lipid Bilayers and Protein Assemblies Supported on Rough Surfaces by Atomic Force Microscopy. *Langmuir* **2003**, *19*, 1632–1640.

(17) Marra, J.; Israelachvili, J. Direct Measurements of Forces between Phosphatidylcholine and Phosphatidylethanolamine Bilayers in Aqueous Electrolyte Solutions. *Biochemistry* **1985**, *24*, 4608–4618.

(18) Orozco-Alcaraz, R.; Kuhl, T. L. Impact of Membrane Fluidity on Steric Stabilization by Lipopolymers. *Langmuir* **2012**, *28*, 7470–7475.

(19) Moore, N. W.; Kuhl, T. L. Bimodal Polymer Mushrooms: Compressive Forces and Specificity toward Receptor Surfaces. *Langmuir* **2006**, *22*, 8485–8491.

(20) Helm, C. A.; Israelachvili, J. N.; McGuiggan, P. M.; ROLE, O. F. Hydrophobic Forces in Bilayer Adhesion and Fusion. *Biochemistry* **1992**, *31*, 1794–1805.

(21) Leckband, D. E.; Helm, C. A.; Israelachvili, J. Role of Calcium in the Adhesion and Fusion of Bilayers. *Biochemistry* **1993**, *32*, 1127–1140.

(22) Sheth, S. R.; Leckband, D. Measurements of Attractive Forces between Proteins and End-Grafted Poly(ethylene glycol) Chains. *Proc. Natl. Acad. Sci. U.S.A.* **1997**, *94*, 8399–8404.

(23) Anderson, T. H.; Min, Y.; Weirich, K. L.; Zeng, H.; Fygenson, D.; Israelachvili, J. N. Formation of Supported Bilayers on Silica Substrates. *Langmuir* **2009**, *25*, 6997–7005.

(24) Sackmann, E. Supported Membranes: Scientific and Practical Applications. *Science* **1996**, *271*, 43–48.

(25) Tamm, L. K.; McConnell, H. M. Supported Phospholipid Bilayers. *Biophys. J.* **1985**, *47*, 105–113.

(26) Siegel, D. P. Inverted Micellar Intermediates and the Transitions between Lamellar, Cubic, and Inverted Hexagonal Lipid Phases. II. Implications for Membrane-Membrane Interactions and Membrane Fusion. *Biophys. J.* **1986**, *49*, 1171–1183.

(27) Paulsson, M. Basement Membrane Proteins: Structure, Assembly, and Cellular Interactions. *Crit. Rev. Biochem. Mol. Biol.* **1992**, *27*, 93–127.

(28) Lorenza, B.; Keller, R.; Sunnicka, E.; Geila, B.; Janshoff, A. Colloidal Probe Microscopy of Membrane–Membrane Interactions: From Ligand–Receptor Recognition to Fusion Events. *Biophys. Chem.* **2010**, *150*, 54–63.

(29) Tanaka, M. S., E. Polymer-Supported Membranes as Models of the Cell Surface. *Nature* **2005**, *437*, 656–663.

(30) Knoll, W.; Bender, K.; Förch, R.; Frank, C.; Götz, H.; Heibel, C.; Jenkins, T.; Jonas, U.; Kibrom, A.; Kügler, R. Polymer-Tethered Bimolecular Lipid Membranes. *Polym. Membr. Biomembr.* **2010**, *224*, 87–111.

(31) Spinke, J.; Yang, J.; Wolf, H.; Liley, M.; Ringsdorf, H.; Knoll, W. Polymer-Supported Bilayer on a Solid Substrate. *Biophys. J.* **1992**, *63*, 1667.

(32) Chi, L.; Anders, M.; Fuchs, H.; Johnston, R.; Ringsdorf, H. Domain Structures in Langmuir-Blodgett Films Investigated by Atomic Force Microscopy. *Science* **1993**, *259*, 213.

(33) Majewski, J.; Wong, J. Y.; Park, C. K.; Seitz, M.; Israelachvili, J. N.; Smith, G. S. Structural Studies of Polymer-Cushioned Lipid Bilayers. *Biophys. J.* **1998**, *75*, 2363–2367.

(34) Wong, J. Y.; Majewski, J.; Seitz, M.; Park, C. K.; Israelachvili, J. N.; Smith, G. S. Polymer-Cushioned Bilayers. I. A Structural Study of Various Preparation Methods Using Neutron Reflectometry. *Biophys. J.* **1999**, *77*, 1445–1457.

(35) Baumgart, T.; Offenhäusser, A. Polysaccharide-Supported Planar Bilayer Lipid Model Membranes. *Langmuir* **2003**, *19*, 1730−1737.
(36) Wang, L.; Schönhoff, M.; Möhwald, H. Lipids Coupled to Polyelectrolyte Multilayers: Ultraslow Diffusion and the Dynamics of Electrostatic Interactions. *J. Phys. Chem. B* **2002**, *106*, 9135−9142.
(37) Smith, H. L.; Jablin, M. S.; Vidyassagar, A.; Saiz, J.; Watkins, E.; Toomey, R.; Hurd, A. J.; Majewski, J. Model Lipid Membranes on a Tunable Polymer Cushion. *Phys. Rev. Lett.* **2009**, *102*, 228102.
(38) Wagner, M. L.; Tamm, L. K. Tethered Polymer-Supported Planar Lipid Bilayers for Reconstitution of Integral Membrane Proteins: Silane-Polyethyleneglycol-Lipid as a Cushion and Covalent Linker. *Biophys. J.* **2000**, *79*, 1400−1414.
(39) Naumann, C.A.; Prucker, O.; Lehmann, T.; Rühe, J.; Knoll, W.; Frank, C. W. The Polymer-Supported Phospholipid Bilayer: Tethering as a New Approach to Substrate-Membrane Stabilization. *Biomacromolecules* **2002**, *3*, 27−35.
(40) Sinner, E.-K.; Knoll, W. Functional Tethered Membranes. *Curr. Opin. Chem. Biol.* **2001**, *5*, 705−711.
(41) El-khouri, R. J.; Bricarello, D. A.; Watkins, E. B.; Kim, C. Y.; Miller, C. E.; Patten, T. E.; Parikh, A. N.; Kuhl, T. L. pH Responsive Polymer Cushions for Probing Membrane Environment Interactions. *Nano Lett.* **2011**, *11*, 2169−2172.
(42) Vigil, G.; Xu, Z.; Steinberg, S.; Israelachvili, J. Interactions of Silica Surfaces. *J. Colloid Interface Sci.* **1994**, *165*, 367−385.
(43) Kuhl, T. L.; Leckband, D. E.; Lasic, D. D.; Israelachvili, J. N. Modulation of Interaction Forces between Bilayers Exposing Short-Chained Ethylene Oxide Headgroups. *Biophys. J.* **1994**, *66*, 1479−1487.
(44) Kuhl, T. L.; Leckband, D. E.; Lasic, D. D.; Israelachvili, J. N. Modulation and Modeling of Interaction Forces between Lipid Bilayers Exposing Terminally Grafted Polymer Chains. In *Stealth Liposomes*; Lasic, D., Martin, F., Ed.; CRC Press: Boca Raton, FL, 1995; pp 73−91.
(45) Klopfer, K. J.; Vanderlick, T. K. Isotherms of Dipalmitoylphosphatidylcholine (DPPC) Monolayers: Features Revealed and Features Obscured. *J. Colloid Interface Sci.* **1996**, *182*, 220−229.
(46) Israelachvili, J. N.; Adams, G. E. Measurement of Forces between Two Mica Surfaces in Aqueous Electrolyte Solutions in the Range 0−100 nm. *J. Chem. Soc., Faraday Trans.* **1978**, *74*, 975−1001.
(47) Israelachvili, J. Thin Film Studies Using Multiple Beam Interferometry. *J. Colloid Interface Sci.* **1973**, *44*, 259.
(48) Moore, N. W.; Mulder, D. J.; Kuhl, T. L. Adhesion from Tethered Ligand-Receptor Bonds with Microsecond Lifetimes. *Langmuir* **2008**, *24*, 1212−1218.
(49) Valle-Delgado, J. J.; Molina-Bolivar, J. A.; Galisteo-Gonzalez, F.; Galvez-Ruiz, M. J.; Feiler, A. Hydration Forces between Silica Surfaces: Experimental Data and Predictions from Different Theories. *J. Chem. Phys.* **2005**, *123*, 3.
(50) Drelich, J.; Long, J.; Xu, Z.; Masliyah, J.; White, C. L. Probing Colloidal Forces between a Si_3N_4 AFM Tip and Single Nanoparticles of Silica and Alumina. *J. Colloid Interface Sci.* **2006**, *303*, 627−638.
(51) Grabbe, A.; Horn, R. G. Double-Layer and Hydration Forces Measured between Silica Sheets Subjected to Various Surface Treatments. *J. Colloid Interface Sci.* **1993**, *157*, 375−383.
(52) Scales, P. J.; Grieser, F.; Healy, T. W.; White, L. R.; Chan, D. Y. C. Electrokinetics of the Silica-Solution Interface: A Flat Plate Streaming Potential Study. *Langmuir* **1992**, *8*, 965−974.
(53) Schwer, C.; Kenndler, E. Electrophoresis in Fused-Silica Capillaries: The Influence of Organic Solvents on the Electroosmotic Velocity and the Zeta Potential. *Anal. Chem.* **1991**, *63*, 1801−1807.
(54) Valtiner, M.; Banquy, X.; Kristiansen, K.; Greene, G. W.; Israelachvili, J. N. The Electrochemical Surface Forces Apparatus: The Effect of Surface Roughness, Electrostatic Surface Potentials, and Anodic Oxide Growth on Interaction Forces, and Friction between Dissimilar Surfaces in Aqueous Solutions. *Langmuir* **2012**, *28*, 13080−13093.
(55) Valtiner, M.; Kristiansen, K.; Greene, G. W.; Israelachvili, J. N. Effect of Surface Roughness and Electrostatic Surface Potentials on Forces Between Dissimilar Surfaces in Aqueous Solution. *Adv. Mater.* **2011**, *23*, 2294−2299.
(56) Castellana, E. T.; Cremer, P. S. Solid Supported Lipid Bilayers: From Biophysical Studies to Sensor Design. *Surf. Sci. Rep.* **2006**, *61*, 429−444.
(57) Tanford, C. Micelle Shape and Size. *J. Phys. Chem.* **1972**, *76*, 21.
(58) Small, D. M. Phase Equilibria and Structure of Dry and Hydrated Egg Lecithin. *J. Lipid Res.* **1967**, *8*, 551−557.
(59) Kuhl, T. L.; Berman, A. D.; Hui, S. W.; Israelachvili, J. N. Part 1. Direct Measurement of Depletion Attraction and Thin Film Viscosity between Lipid Bilayers in Aqueous Polyethylene Glycol Solutions. *Macromolecules* **1998**, *31*, 8250−8257.
(60) Pincet, F.; Cribier, S.; Perez, E. Bilayers of Neutral Lipids Bear a Small but Significant Charge. *Eur. Phys. J. B* **1999**, *11*, 127−130.
(61) Giasson, S.; Kuhl, T. L.; Israelachvili, J. N. Adsorption and Interaction Forces of Micellar and Microemulsion Solutions in Ultrathin Films. *Langmuir* **1998**, *14*, 891−898.
(62) Tristram-Nagle, S.; Petrache, H. I.; Nagle, J. F. Structure of Fully Hydrated Bilayer Dispersions. *Biochim. Biophys. Acta* **1988**, *942*, 1−10.
(63) Watkins, E. B.; Miller, C. E.; Mulder, D. J.; Kuhl, T. L.; Majewski, J. Structure and Orientational Texture of Self-Organizing Lipid Bilayers. *Phys. Rev. Lett.* **2009**, *102*, 238101.
(64) Bassereau, P.; Pincet, F. Quantitative Analysis of Holes in Supported Bilayers Providing the Adsorption Energy of Surfactants on Solid Substrate. *Langmuir* **1997**, *13*, 7003−7007.
(65) Duncan, S. L.; Larson, R. G. Comparing Experimental and Simulated Pressure-Area Isotherms for DPPC. *Biophysics* **2008**, *94*, 2965−2986.
(66) Ma, G.; Allen, H. C. DPPC Langmuir Monolayer at the Air-Water Interface: Probing the Tail and Head Groups by Vibrational Sum Frequency Generation Spectroscopy. *Langmuir* **2006**, *22*, 5341−5349.
(67) Van Oss, C. J. *Interfacial Forces in Aqueous Media*; Marcel Dekker: New York, 1994.
(68) Dufrene, Y. F.; Lee, G. U. Advances in the Characterization of Supported Lipid Films with the Atomic Force Microscope. *Biochim. Biophys. Acta, Biomembr.* **2000**, *1509*, 14−41.
(69) Hui, S. W.; Viswanathan, R.; Zasadzinski, J. A.; Israelachvili, J. N. The Structure and Stability of Phospholipid-Bilayers by Atomic-Force Microscopy. *Biophys. J.* **1995**, *68*, 171−178.